SI Appendix

Title:
Nitrate modulates stem cell dynamics in *Arabidopsis* shoot meristems through cytokinins

Authors:
Benoit Landrein[a], Pau Formosa-Jordan[a], Alice Malivert[a,b], Christoph Schuster[a], Charles W. Melnyk[a,c], Weibing Yang[a], Colin Turnbull[d], Elliot M. Meyerowitz[a,e], James C.W. Locke[a,f], Henrik Jönsson[a,g,h]

Author Affiliations:
[a] Sainsbury Laboratory, University of Cambridge, Bateman Street, Cambridge, CB2 1LR, UK; [b] École Normale Supérieure de Lyon, Université Claude Bernard Lyon I, Université de Lyon, 69342 Lyon Cedex 07, France; [c] Department of Plant Biology, Swedish University of Agricultural Sciences, Almas allé 5, 756 51, Uppsala, Sweden; [d] Department of Life Sciences, Imperial College London, London SW7 2AZ, UK; [e] Howard Hughes Medical Institute and Division of Biology and Biological Engineering, California Institute of Technology, Pasadena, CA 91125, USA; [f] Microsoft Research, Cambridge CB1 2FB, UK; [g] Computational Biology and Biological Physics Group, Department of Astronomy and Theoretical Physics, Lund University, S-221 00 Lund, Sweden; [h] Department of Applied Mathematics and Theoretical Physics, University of Cambridge, Cambridge CB3 0DZ, UK.

Correspondence:
Henrik Jönsson, Sainsbury Laboratory, University of Cambridge, Bateman Street, Cambridge CB2 1LR, UK, tel.: + 44 (0)1223 761128, henrik.jonsson@slcu.cam.ac.uk
James C.W. Locke, Sainsbury Laboratory, University of Cambridge, Bateman Street, Cambridge CB2 1LR, UK, tel. + 44 (0)1223 761110, james.locke@slcu.cam.ac.uk
Elliot M. Meyerowitz, Howard Hughes Medical Institute and Division of Biology and Biological Engineering, California Institute of Technology, Pasadena, CA 91125, USA, tel. +1 (626) 395-6889, meyerow@caltech.edu

Keywords:
Arabidopsis | shoot apical meristem | plant nutrition | plant development | cytokinin hormones

SI Materials and Methods

Plant Materials:
Col-0 seeds were provided by the Salk stock center. The *pCLV3::dsRED* and *pWUS::GFP* marker lines were previously described (1, 2). The *pTCS::GFP* marker was provided by Teva Vernoux (3), and the *pTCSn::GFP* was provided by Bruno Müller (4). The *WUS-GFP* marker complementing the *wus* mutant phenotype was provided by Jan Lohmann (5). The triple *ipt* mutant *ipt3-1; ipt5-2; ipt7-1* (*ipt3.5.7*) was provided by Ottoline Leyser (6). The *log4-3; log7-1* (*log4.7*), *log1-2; log3-2; log4-3; log7-1* (*log1.3.4.7*) and *cyp735a1-1; cyp735a2-1 (cyp735a1.2)* mutant seeds were provided by Hitoshi Sakakibara and the RIKEN Institute (7, 8). The *ckx3-1* (SAIL_55_G12/CS870580); *ckx5-2* (Salk_117512C) double mutant has already been described (9) and was generated by Paul Tarr.

Growth conditions:
For all plants grown on soil, batches of seeds were dispersed in pots of soil (Levington F2) and placed for 3 days in a 4°C room for stratification and 7 days in a short day room (8h light) for germination. Seedlings were transferred into separate pots containing different mixes of sand (Royal Horticultural Society: Silver Sand) and soil (Levington F2) and put into a constant light room (24 h light, temperature: 22°C, light intensity 160 µmol m^{-2} s^{-1}). Plants were watered without or with 1/1/1 fertilizer (Vitafeed Standard). The experiments were carried out at the beginning of the flowering stage when the main inflorescence stem was no more than few centimetres in height.

For the nitrate resupply experiment, seedlings were germinated on soil and put in a short day room (8h light) for 7 days after stratification before being transferred into small individual pots of ½ sand (Leighton Buzzard sand from WBB Minerals) ½ Terra-green (Oil-Dri) pre-watered with 25 mL of an ATS-derived (*Arabidopsis* salts medium) nutritive solution containing 1.8 mM of NO_3 prepared by adjusting the concentrations of the following components: 0.4 mM $Ca(NO_3)_2$, 1 mM KNO_3, 4 mM KCl and 1.6 mM $CaCl_2$ (10, 11). Plants were put for 2 weeks in a short day room (8h light) before being transferred into a constant light room. Each plant was fed weekly with 10 mL of the same nutrient solution. The experiments were carried out at the beginning of the flowering stage when the main inflorescence stem was of few centimetres in height. At the beginning of the experiment (at day 0), plants were randomized, separated into three populations and watered with 25 mL of the nutritive solution containing either 0 mM of NO_3 (by adjusting the concentrations of the following components: 0 mM $Ca(NO_3)_2$, 0 mM KNO_3, 5 mM KCl and 2 mM $CaCl_2$), 1.8 mM of NO_3 (same solution as described earlier) or 9 mM of NO_3 (normal ATS solution). Each day, 5-10 new plants were used for analysis.

Within the course of the experiments, we realized that the tap water used for watering the plants contained non-negligible levels of NO_3 (up to 0.7 mM in the summer), which could have moderately influenced our measurements and explain some of the differences observed between experimental repeats. Note however that within an experimental repeat, all genotypes or conditions were grown simultaneously and experienced the same growth conditions.

Analysis of the content of mineral nutrients in the soil
WT plants were grown in three types of soil as described above (½Soil and ½ Sand, 1/1 Soil, 1/1 Soil + Fertilizer). At bolting stage, the plants were removed, and the soil was harvested after manual exclusion of as much of the roots as possible. Analysis was performed by NRM laboratories (http://www.nrm.uk.com/services.php?service=horticulture).

Generation of the *p35S::XVE-IPT3-TFP* line:
The coding sequence of *IPT3* was amplified from Col-0 cDNA (primers: F: TTTGGATCCTATG-ATCATGAAGATATCTATGGCTATG and R: AATGAATTCTCGCCACTAGACACCGCGAC) and put by conventional cloning into a pENTR1Ad modified vector containing a synthetic sequence for a GS repeat linker peptide of 30 amino acids identical to the one described in (5). Then, a LR recombination was performed using the *p35S::XVE-pENTR-R4-L1* plasmid described in (12) and kindly provided by Ari-Pekka Mähönen, the *pENTR1Ad-IPT3-linker*, *TFP-pENTR-R2-L3* (Turquoise fluorescent protein) and the *pH7m34GW* destination vector coding for hygromycine resistance. The resulting plasmid was transformed into *Arabidopsis* plants carrying either both *pTCS::GFP* and *pCLV3::dsRED* or *pWUS::GFP* by flower dip transformation. Although we could see the effect of inducing *IPT3-TFP* in multiple independent insertions for each marker, we could only observe a very weak TFP signal by confocal microscopy.

Image acquisition and time-lapse:
Imaging was performed as follows: first, the main inflorescence meristem of plants at the beginning of the flowering stage was cut one to two centimeters from the tip, dissected under a binocular stereoscopic microscope to remove all the flowers older than stage 3 (as defined in (13)) and transferred to a box containing an apex culture medium (ACM) with vitamins as described in (14). Meristems were imaged in water using a 20X long-distance water-dipping objective mounted either on a LSM700 or a LSM780 confocal microscope (Zeiss, Germany). Z-stacks of 1 or 2 µm spacing were taken. In some experiments, meristems were put in contact with a solution of 0.1 mg/mL of FM4-64 (Thermo-Fisher) for 10 minutes and washed in sterile water prior to imaging to dye the cell membranes. For the time-lapse experiments looking at the effect of extrinsic cytokinin, meristems were put in a box of ACM with vitamins and without or with 50µM of tZR or of tZ (Sigma) diluted from 50mM stock solutions. To prepare those stock solutions, tZR was dissolved in 10mM NaOH and tZ in 100% DMSO. Control meristems were incubated with a similar volume of both NaOH and DMSO. Meristems were kept in a constant light phytotron and covered with the same solution of liquid ACM for imaging. For the time-lapse experiment looking at the effect of an estradiol-based induction of *IPT3*, meristems were put in a box of ACM with vitamins and with 5 µM of β-estradiol (Sigma) or with the equivalent volume of DMSO as a control. Again, meristems were kept in a constant light phytotron and covered with the same liquid ACM solution for imaging.

Image Analysis:
Confocal stacks were analyzed using the ImageJ software (https://fiji.sc/). Z-projections (maximum intensity) of the stacks were performed to analyze meristems dyed with FM4-64. Z-projections (sum slices) of the stacks were performed to analyze meristems expressing *GFP* or its derivatives and the "fire" lookup table was used to represent the signal. Meristem size and plastochron ratio were measured as described in (15). Note that as the plastochron ratio is the average area between successive primordia, this parameter is more variable for meristems producing few organs as it is averaged on a smaller number of measurements. The expression level and domain size of the *pTCSn::*GFP, pWUS*::GFP*, *WUS-GFP* and *pCLV3::dsRED* were analyzed using a Matlab pipeline (Mathworks Inc., Natick, MA) specifically developed for this study (see below).

Characterization of gene expression domains through automated image analysis:
In order to characterize quantitatively the *WUS-GFP*, *pWUS::GFP*, *pTCSn::GFP* and *pCLV3::dsRED* domains in meristems, we developed an automatic pipeline with custom-made code written in Matlab. The code performs two basic tasks: first, it automatically identifies the fluorescent domain in the inflorescence meristem. Second, it computes the size and the intensity of such a domain. Domain

identification is performed on a Gaussian filtered (σ=5μm) maximal intensity projection of the fluorescence image under study, while the size and intensity of the domain calculation is performed on a Gaussian filtered (σ=5μm) sum-slice projection. In both tasks, the Gaussian filter is used to smooth out the fluorescence images so that we neutralize the intracellular localization (ER or nucleus) of the fluorescent markers. This produces a more continuous fluorescence domain, which facilitates the automated extraction of its main features. Below, we explain in further detail how this pipeline was structured and used.

The automatic identification of the center of *WUS* and *CLV3* expression domains is performed through an Otsu thresholding over the corresponding z-projected and Gaussian-filtered fluorescence images. As floral primordia also express the reporters, it is assumed that the expression domain of the inflorescence meristem is the one that is the closest to the center of each image. Then, the centroid, $\boldsymbol{r_0}$, of this domain is found and a circular region R of radius ρ_R=40 μm is defined that should contain the fluorescence domain under study in the meristem. In the cases where the expression domain has failed to be automatically detected – e.g., in those images where the meristem was not well centered – we have manually specified the center of the inflorescence meristem.

After domain detection, the size of fluorescence domains is determined. To do so, the radially symmetric decay of the fluorescence in the R regions of the corresponding z-projected and Gaussian filtered images is characterized. Specifically, a characteristic length L_0 of such decay in each R region is extracted, and we interpret this as the fluorescence characteristic domain size. To extract L_0, the mean fluorescence intensity within different concentric subregions within region R around the centroid $\boldsymbol{r_0}$ is computed; the most central subregion is a circle of radius $d\rho$=1 μm, and the other subregions are 39 concentric i-toroids ($i=1,\ldots,39$) filling the R region; the i-th toroid is defined by those pixels whose (x,y) coordinates fulfill the relation $\rho_i^2<(x-x_0)^2+(y-y_0)^2\leq\rho_{i+1}^2$, x_0 and y_0 being the coordinates of the centroid $\boldsymbol{r_0}$ and where $\rho_i=id\rho$. Then, the characteristic length L_0 is extracted by fitting the fluorescence profile to an exponential function of the form (16)

$$F(r) = C_0 + C_1 e^{-\left(\frac{r}{L_0}\right)^n} , \qquad (1)$$

where C_0 corresponds to the mean autofluorescence levels of the sum slices projection, C_1 is the height of the fluorescent peak, and n is an exponent accounting for the radial decay of the fluorescent domain. C_0, C_1 and n are also determined in the fit.

The total fluorescence of the selected domains (referred as signal), M_R, is calculated by

$$M_R = \gamma \sum_{j\in R} p_j , \qquad (2)$$

where p_j is the pixel intensity levels in the j-th pixel of the sum slices projection, and γ is the resolution in microns squares of the image under study. The γ factor corrects the differences in intensity levels between images that have different resolution. Then, the inferred autofluorescence, B_R, is subtracted from the summed fluorescence in the selected domain, so that the intensity used in the analysis reads

$$I_R = M_R - B_R , \qquad (3)$$

where $B_R=C_0A_R$, being A_R the area of the R region.

We have checked that when fixing the n exponent as the average exponent for all the meristems in a given experiment, we obtained equivalent results for the characteristic length and total fluorescence to the case where the n exponent was a free parameter.

The code can be found following this link: https://gitlab.com/slcu/teamHJ/pau/RegionsAnalysis (v0.1).

RNA extraction and qPCR:

Three biological replicates of three roots each were used in each time-point. Roots were quickly washed in water to remove the sand and terra-green and frozen in liquid nitrogen before being manually ground. Total RNA was extracted using the RNA plus mini kit (Qiagen). First strand cDNA was then synthesized using the Transcriptor First strand cDNA kit (v.6, Roche). Real-time quantitative PCR was performed using double-strand DNA-specific dye SYBR Green (Applied Biosystems) in a LightCycler 480 II (Roche). Three positive replicates and one negative (using as template a product of the cDNA transcription made without the transcriptase) were performed for each reaction. Expression of *UBQ10*, *NIA1*, *IPT3* and *IPT5* was assessed using the primers described in the following table. Expression data of *NIA1*, *IPT3* and *IPT5* were obtained by normalizing for each replicate the ½ CT of the corresponding gene by the one of *UBQ10*.

UBQ10-qPCR-F	AACTTTGGTGGTTTGTGTTTTGG
UBQ10-qPCR-R	TCGACTTGTCATTAGAAAGAAAGAGATAA
NIA1-qPCR-F	GCACGTTTTCGTTTGCGC
NIA1-qPCR-R	GATATGACCAACCGCGTCG
IPT3-pPCR-F	AGACTTCCCTCCAGCGAGAT
IPT3-qPCR-R	GAGAGTCGTGACTTGCCTGT
IPT5-qPCR-F	ACCTAGCCACTCGTTTTCCG
IPT5-qPCR-R	TTCGTAAGTGTCGTGGACGG

Cytokinin analysis by mass spectrometry:

Three replicates of three roots, shoots or inflorescences each were used in each condition. Tissues were frozen in liquid nitrogen, ground manually and an aliquot of 100 to 400 mg was taken and weighed. Cytokinins were then extracted and measured by liquid chromatography - mass spectrometry (LC-MS) following the protocol described in (17), with the following modifications: the mass spectrometer was an Applied Biosystems QTrap 6500 system, and the initial mobile phase was 5% acetonitrile in 10 mM ammonium formate (pH3.4). Note that differences in the level of cytokinin species observed between the two experiments presented in *SI Appendix* Fig. S8, Table S2 and Table S3 are partly attributable to lower amounts of recovered standards that precluded accurate measurement of all the glucoside species in the second replicate. Although the experiments had a similar design, it may also be that subtle variations in plant growth lead to slightly different overall CK profiles.

Grafting:

Arabidopsis micro-grafting was performed on 7-day-old seedlings according to the protocol described in (18). Grafted seedlings were transferred to soil 7 days after grafting, watered with 1/1/1 fertilizer and put in a constant light room until bolting stage.

In situ Hybridization

Full length *WUS* cDNA was amplified by PCR using specific primers and ligated into a pGEM-T Easy vector (Promega). Transcription was performed using the DIG RNA labelling kit (Roche). Embedding of the samples, sectioning (8 μm sections) and in situ hybridization were performed following the protocol described in (http://www.its.caltech.edu/~plantlab/ protocols/insitu.pdf) with the addition of 4% polyvinyl alcohol (PVA) to the nitro blue tetrazolium-bromochloroindolyl phosphate (NBT-BCIP) staining solution. Sections were captured with a 20x lens using an Axioimager microscope (Zeiss) with fully opened diaphragm at 2048 x 2048 picture size. Quantification of the *WUS* expression area was described previously (19). The threshold was determined by the mean intensity of the unstained tissue of the same section minus four standard deviations. Three consecutive sections that showed the strongest staining signal were analyzed per meristem and the expression area was averaged. For *ipt3.5.7*

and *cyp735a1.2*, the staining signal of two consecutive sections was quantified and averaged, since *WUS* signal was only detectable in two sections. Image analysis was performed using the ImageJ software.

Statistical analysis

Statistical analyses were performed using either Microsoft Excel or R software (https://www.R-project.org). Mean or mode values (for boxplots) are shown with error bars corresponding either to the standard deviation or the standard error (specified in the legend of each figure). In the boxplots, the ends of the box also show the upper and lower quartiles. The number of biological repeats (number of plants) is displayed in the legend of each figure or within the figure itself. When applicable, data were fitted using linear models. Student's t-tests were performed to compare time points and genotypes. The measurements were assumed to have two-tailed distributions and unequal variances and were considered as significantly different when the p-value was lower than 0.05.

Each experiment was carried out two times independently except the qPCR analysis and the measurement of cytokinin levels in the transient nitrate treatment. The results of two independent experiments were pooled except in the two following cases. When the fluorescence of an image obtained by confocal microscopy was quantified without normalization, independent experiments could not be pooled as there were fluctuations in the intensity of the laser of the microscope over extended periods of time even if the same microscopy settings are applied (Fig. 2, and *SI Appendix*, Figs. S3 to S5). In the transient nitrate treatments, independent experiments could not be pooled because batches of plants growing on a low concentration of NO_3 were not necessarily of comparable sizes before the beginning of the experiment (as seen by their difference of meristem size at day 0), at least partly because of the seasonality in the levels of nitrate in the tap water (Fig. 6, and *SI Appendix*, Figs. S12 to S15).

Data availability:

The processed confocal z-stacks can be downloaded from Cambridge University D-space Repository (https://www.repository.cam.ac.uk/). Source code for the automatic analysis of gene expression can be found following this link: https://gitlab.com/slcu/teamHJ/pau/RegionsAnalysis (v0.1).

1. Gruel J, *et al.* (2016) An epidermis-driven mechanism positions and scales stem cell niches in plants. *Sci Adv* 2(1):e1500989.
2. Jonsson H, *et al.* (2005) Modeling the organization of the WUSCHEL expression domain in the shoot apical meristem. *Bioinformatics* 21 Suppl 1:i232-240.
3. Besnard F, Rozier F, & Vernoux T (2014) The AHP6 cytokinin signaling inhibitor mediates an auxin-cytokinin crosstalk that regulates the timing of organ initiation at the shoot apical meristem. *Plant Signal Behav* 9(4).
4. Zurcher E, *et al.* (2013) A robust and sensitive synthetic sensor to monitor the transcriptional output of the cytokinin signaling network in planta. *Plant Physiol* 161(3):1066-1075.
5. Daum G, Medzihradszky A, Suzaki T, & Lohmann JU (2014) A mechanistic framework for noncell autonomous stem cell induction in Arabidopsis. *Proc Natl Acad Sci U S A* 111(40):14619-14624.
6. Miyawaki K, *et al.* (2006) Roles of Arabidopsis ATP/ADP isopentenyltransferases and tRNA isopentenyltransferases in cytokinin biosynthesis. *Proc Natl Acad Sci U S A* 103(44):16598-16603.
7. Tokunaga H, *et al.* (2012) Arabidopsis lonely guy (LOG) multiple mutants reveal a central role of the LOG-dependent pathway in cytokinin activation. *Plant J* 69(2):355-365.
8. Kiba T, Takei K, Kojima M, & Sakakibara H (2013) Side-chain modification of cytokinins controls shoot growth in Arabidopsis. *Dev Cell* 27(4):452-461.
9. Melnyk CW, Schuster C, Leyser O, & Meyerowitz EM (2015) A Developmental Framework for Graft Formation and Vascular Reconnection in Arabidopsis thaliana. *Curr Biol* 25(10):1306-1318.

10. Wilson AK, Pickett FB, Turner JC, & Estelle M (1990) A dominant mutation in Arabidopsis confers resistance to auxin, ethylene and abscisic acid. *Mol Gen Genet* 222(2-3):377-383.
11. Muller D, *et al.* (2015) Cytokinin is required for escape but not release from auxin mediated apical dominance. *Plant J* 82(5):874-886.
12. Siligato R, *et al.* (2016) MultiSite Gateway-Compatible Cell Type-Specific Gene-Inducible System for Plants. *Plant Physiol* 170(2):627-641.
13. Smyth DR, Bowman JL, & Meyerowitz EM (1990) Early flower development in Arabidopsis. *Plant Cell* 2(8):755-767.
14. Fernandez R, *et al.* (2010) Imaging plant growth in 4D: robust tissue reconstruction and lineaging at cell resolution. *Nat Methods* 7(7):547-553.
15. Landrein B, *et al.* (2015) Meristem size contributes to the robustness of phyllotaxis in Arabidopsis. *J Exp Bot* 66(5):1317-1324.
16. Bergmann S, *et al.* (2007) Pre-steady-state decoding of the Bicoid morphogen gradient. *PLoS Biol* 5(2):e46.
17. Young NF, *et al.* (2014) Conditional Auxin Response and Differential Cytokinin Profiles in Shoot Branching Mutants. *Plant Physiol* 165(4):1723-1736.
18. Melnyk CW (2017) Grafting with Arabidopsis thaliana. *Methods Mol Biol* 1497:9-18.
19. Geier F, *et al.* (2008) A quantitative and dynamic model for plant stem cell regulation. *PLoS One* 3(10):e3553.

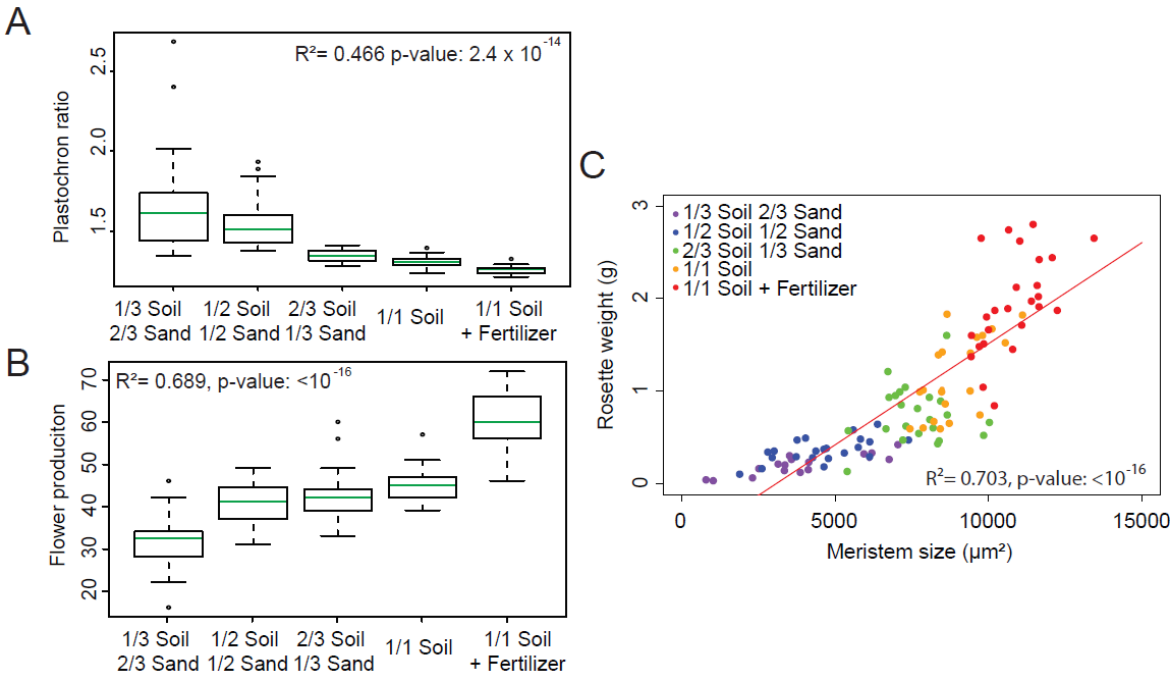

Fig. S1 Plant nutritional status influences meristem function.
(*A*) Plastochron ratio of WT plants grown on soils of different nutritive quality (1/3 soil 2/3 sand: n=17, ½ soil ½ sand: n=22, 2/3 soil 1/3 sand: n=23, 1/1 soil: n=21, 1/1 soil + fertilizer: n=26, pool of 2 independent experiments). Note that as the plastochron ratio is the average area between successive primordia, this parameter is more variable for meristems producing few organs as it is averaged on a smaller number of measurements. Error bars correspond to the mean ± SD. (*B*) Number of flowers produced by the main inflorescence within the first 15 days of flowering of WT plants grown on soils of different nutritive quality (1/3 soil 2/3 sand: n=34, ½ soil ½ sand: n=32, 2/3 soil 1/3 sand: n=33, 1/1 soil: n=34, 1/1 soil + fertilizer: n=18, pool of 2 independent experiments). Error bars correspond to the mean ± SD. (*C*) Correlation between rosette weight and SAM size of WT plants grown on soils of different nutritive quality (n=109, pool of 2 independent experiments). Data were fitted using a linear model.

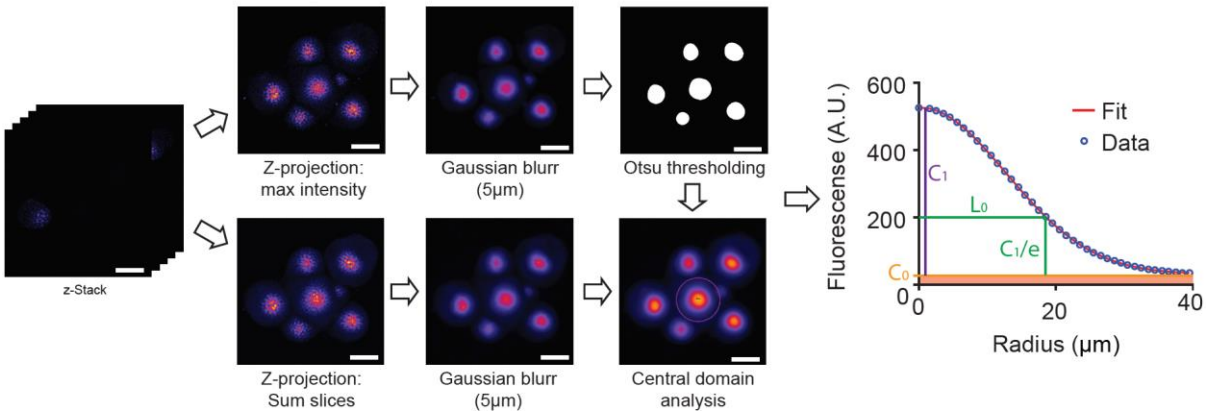

Fig. S2 Automatic analysis of gene expression domains in the SAM.
In order to detect the expression domain, a maximal intensity z-projection of the stack (here from a meristem expressing *WUS-GFP*) is performed and the resulting image is blurred (Gaussian filter of radius: 5 µm). The GFP domain is then automatically detected using a binary transformation of the image resulting from an Otsu thresholding. To extract the size and the total fluorescence level of the detected domain, a blurred (Gaussian filter of radius: 5 µm) z-projection of the stack summing the signal in each slice is performed. Then, the average signal of the domain is extracted at a defined distance from the center of such domain, which shows a curve with a stretched exponential decay. In order to extract the characteristic length of such domain, an exponential fit is applied to the extracted intensity data. The characteristic length of the domain is defined as the domain radius so that the GFP signal – with the autofluorescence levels subtracted - has decreased a factor 1/e from its maximum. Finally, the total GFP signal (after removal of the autofluorescence signal) is then measured. C_0: background signal, C_1: maximum signal without background, L_0: characteristic length, e: e number (See *SI Appendix*, *SI Material and Methods*). Scale bars: 50 µm.

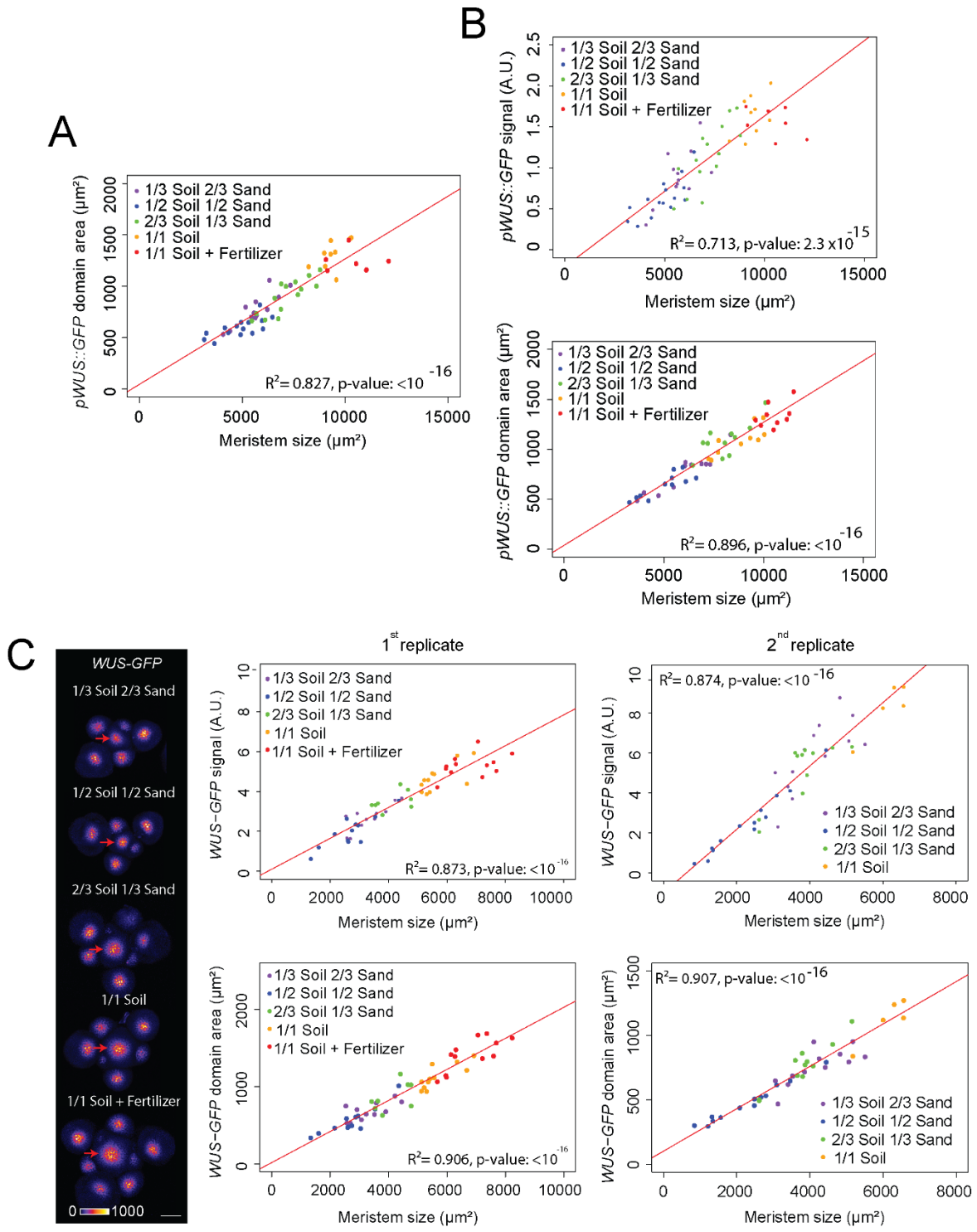

Fig. S3 Plant nutritional status influences *WUS* expression in the SAM.
(*A*) Characteristic size domain of expression of *pWUS::GFP* in WT plants grown on soils of different nutritive quality from the same experiment as Fig. 2*A* (n=57). (*B*) Expression of *pWUS::GFP* in WT plants grown on soils of different nutritive quality from an independent experiment different from the one shown in Fig. 2*A* and *SI Appendix* Fig. S3*A* (n=52). (*C*) Expression of *WUS-GFP* in WT plants grown on soils of different nutritive quality (1st replicate, n=54; 2nd replicate, n=42, scale bar: 50 µm). Red arrows on the left panel point to the center of the SAM. Data were fitted using linear models.

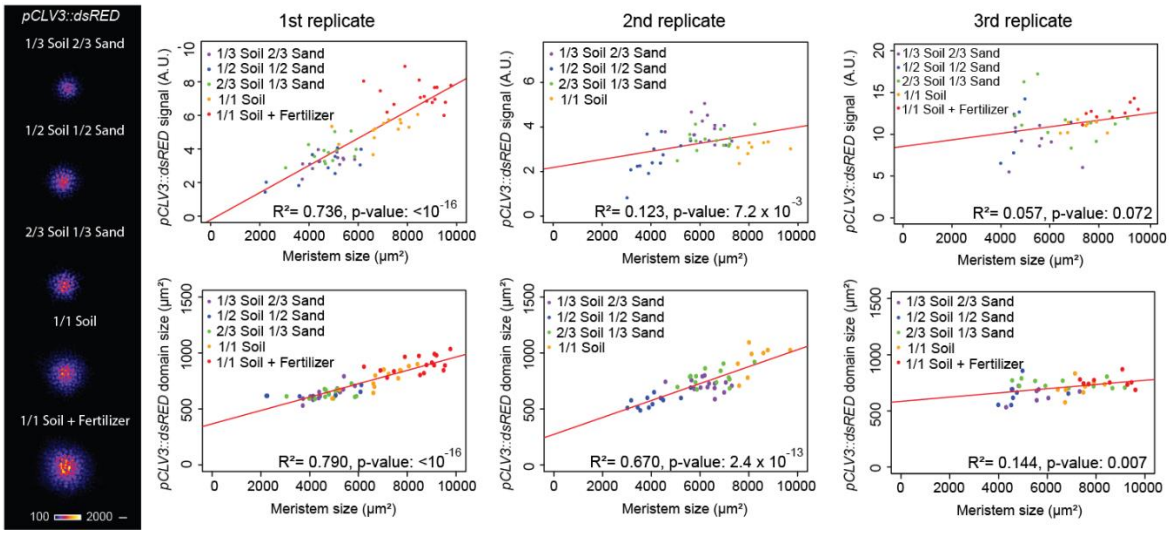

Fig. S4 Plant nutritional status moderately influences *pCLV3::dsRED* expression in the SAM
Expression of *pCLV3::dsRED* in WT plants grown on soils of different nutritive quality (1st replicate: n=65, 2nd replicate: n=50, 3rd replicate: n=44, scale bar: 50 µm). Red arrows point to the center of the SAM. Data were fitted using linear models.

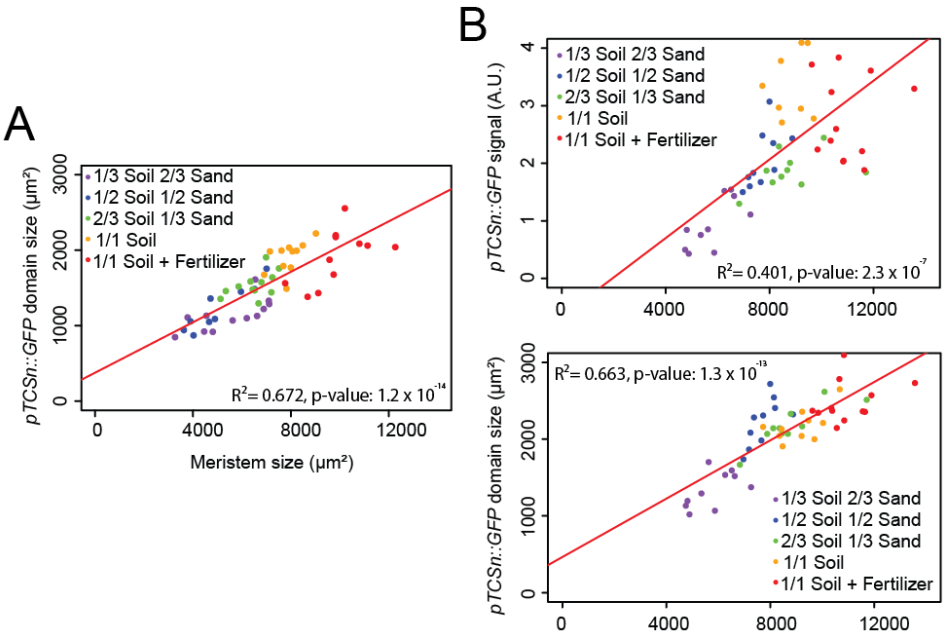

Fig.S5 Plant nutritional status influences cytokinins response in the SAM
(*A*) Characteristic size of the domain of expression of *pTCSn::GFP* in WT plants grown on soils of different nutritive quality from the same experiment as Fig. 2*B* (n=55). (*B*) Expression of *pTCSn::GFP* in WT plants grown on soils of different nutritive quality levels from an independent experiment different from the one shown in Fig. 2*B* and *SI Appendix* Fig. S5*A* (n=52). Top shows total fluorescence signal and bottom shows characteristic size of the domain of expression. Data were fitted using linear models.

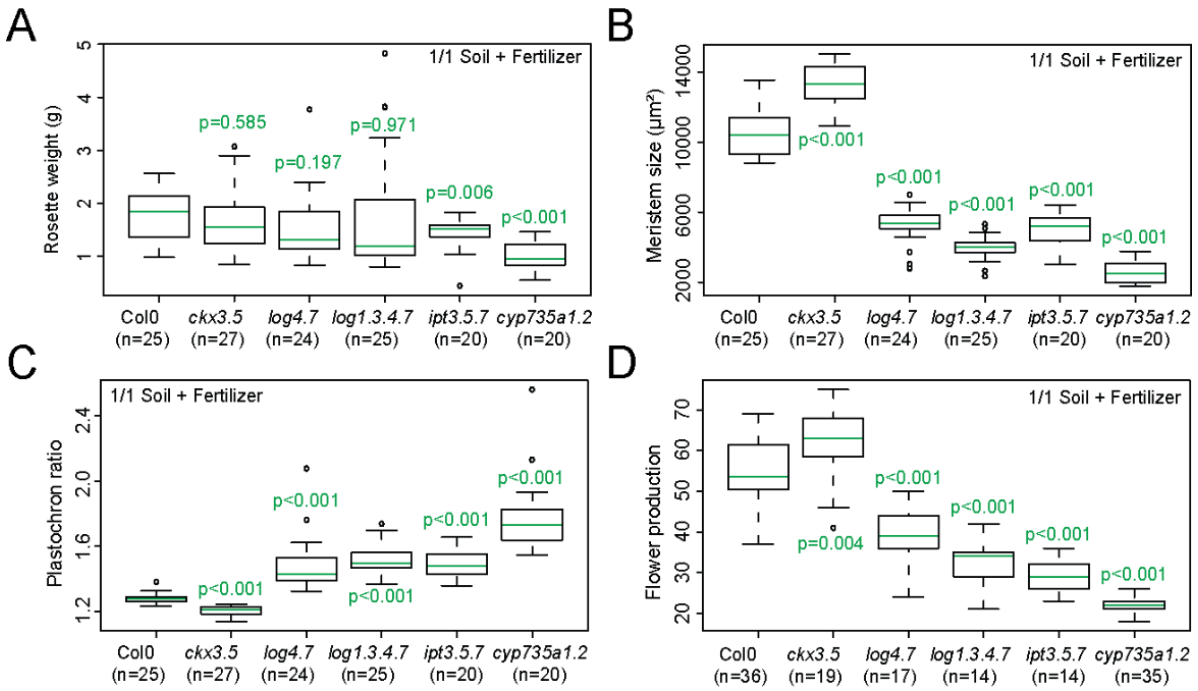

Fig. S6 Phenotype of cytokinin-associated mutants.
Rosette weight at bolting stage (*A*), meristem size (*B*), plastochron ratio (*C*) and number of flowers produced by the main inflorescence within the first 15 days of flowering (*D*) of WT and CK-associated mutants grown on soil with fertilizer (2 independent experiments, the numbers of replicates are displayed in the Figure). Each green p-value corresponds to the result of a Student's t-test between a given mutant and the WT (Col-0). Error bars correspond to the mean ± SD.

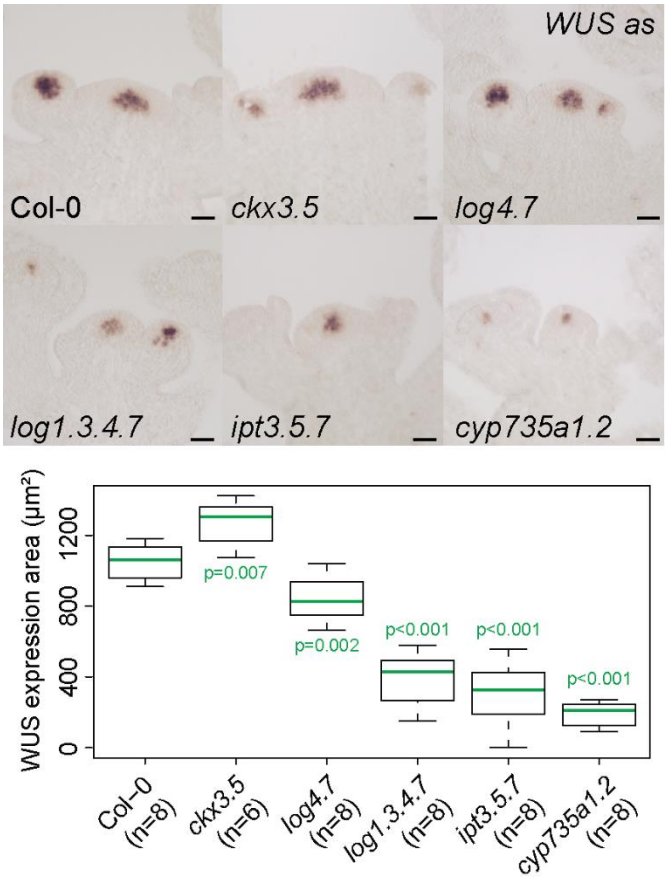

Fig. S7 *WUS* expression is altered in cytokinin-associated mutants

Expression of *WUS* revealed by *in situ* hybridization in meristems of Col-0 wild-type plants and cytokinin-associated mutants at bolting stage and grown on soil with fertilizer (scale bars in the top panel: 10 µm). *WUS* domain sizes in mutants were compared to Col-0 using Welch's t-test (the numbers of replicates are displayed in the Figure). Error bars correspond to the mean ± SD.

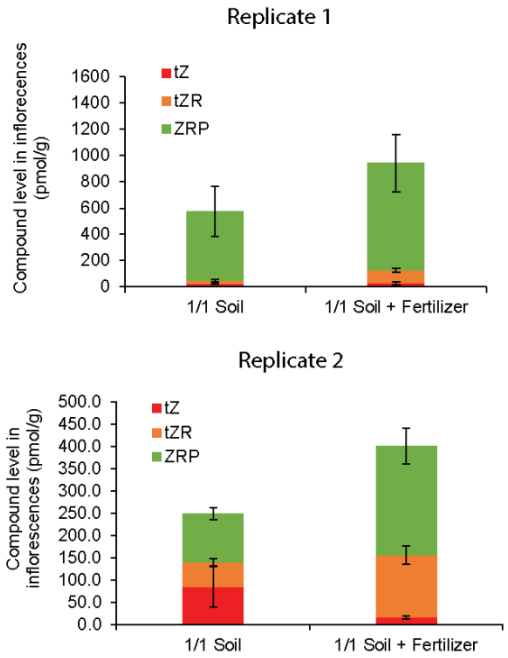

Fig. S8 Plant nutritional status influences cytokinin levels in the inflorescence
Concentration of tZRP, tZR and tZ in inflorescences of plants grown on soil without or with fertilizer in two different experimental repeats and measured by liquid chromatography mass spectrometry (n=3 replicates or 3 inflorescences each). Error bars correspond to the SEM.

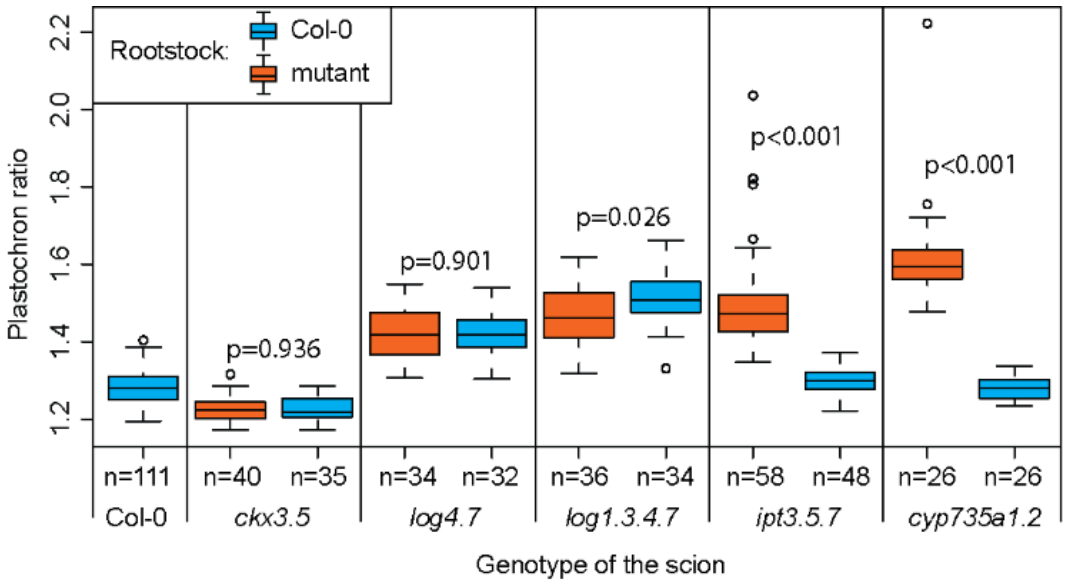

Fig. S9 Plastochron ratio of the inflorescence meristem of WT and cytokinin-associated mutant plants self-grafted or grafted with a WT root and grown in soil supplied with fertilizer (pool of two independent experiments, the numbers of replicates are displayed in the figure). Data were compared using Student's t-test. Error bars correspond to the mean ± SD.

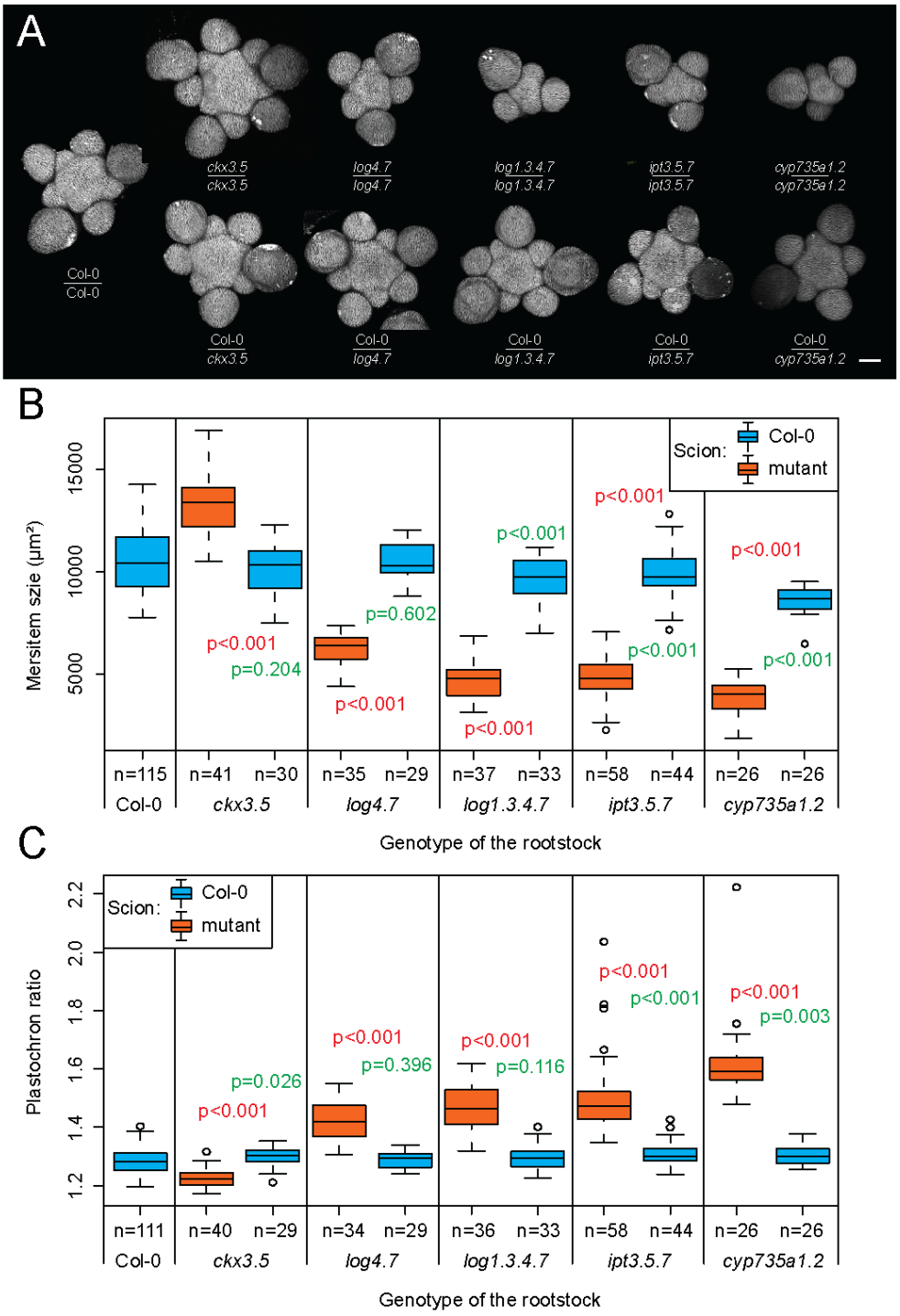

Fig. S10 Cytokinin biosynthesis in the root is not strictly necessary for proper meristem function
(*A*) Meristems of WT and cytokinin-associated mutant plants self-grafted or grafted with a WT rootstock and grown in soil supplied with fertilizer (Scale bar: 50 µm). (*B* and *C*) Meristem size (*B*) and plastochron ratio (*C*) of WT and cytokinin-associated mutant plants self-grafted or grafted with a WT rootstock and grown in soil supplied with fertilizer (pool of two independent experiments, the numbers of replicates are displayed in the figure). Data were compared using Student's t-test, in green is displayed the *p-value* when comparing a given plant graft with the self-grafted WT and in red is displayed the *p*-value when comparing a given plant graft with the corresponding self-grafted mutant. Error bars correspond to the mean ± SD.

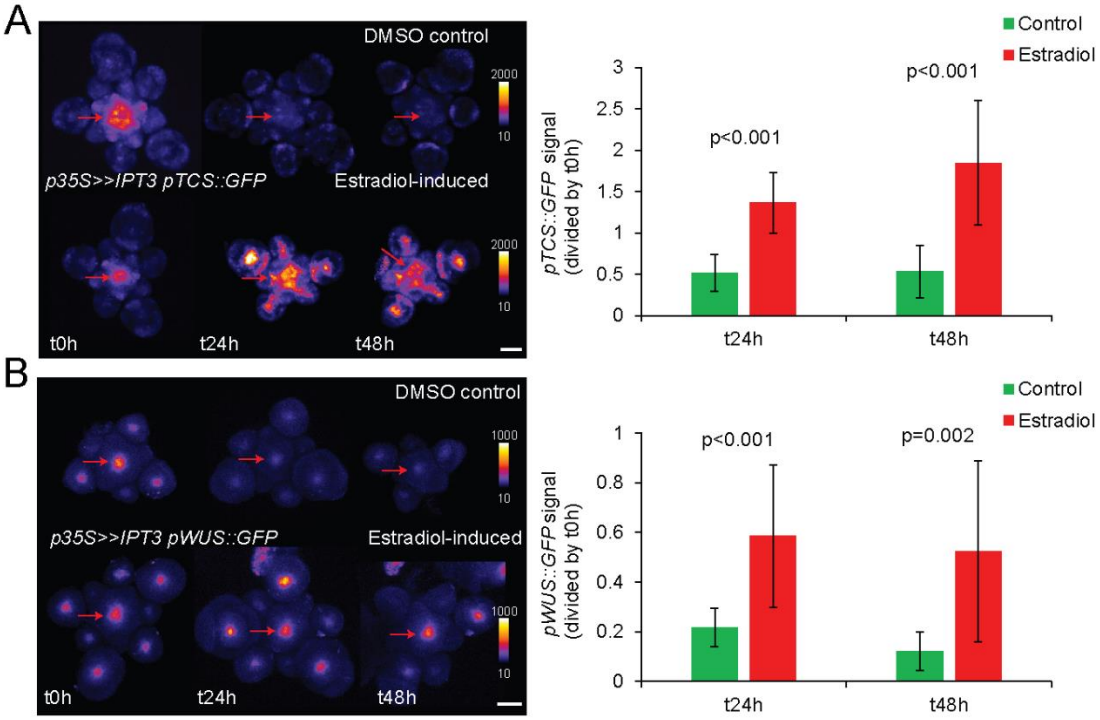

Fig. S11 *IPT3* is sufficient to maintain cytokinin signaling and *WUS* expression *in-vitro*
Effect of an induction of *IPT3* using an estradiol inducible system under the control of the *p35S* on the expression of *pTCS::GFP* (*A*) or p*WUS::GFP* (*B*) in cut meristems grown *in vitro* without addition of extrinsic cytokinin (scale bars: 50 µm, pools of two independent experiments, *pTCS::GFP*: n=17, *pWUS::GFP*: n=12). For each meristem, the signal at 24h and 48h was divided by the signal at 0h. Red arrows point to the center of each inflorescence meristem. Data were compared using Student's t-tests. Error bars correspond to the mean ± SD.

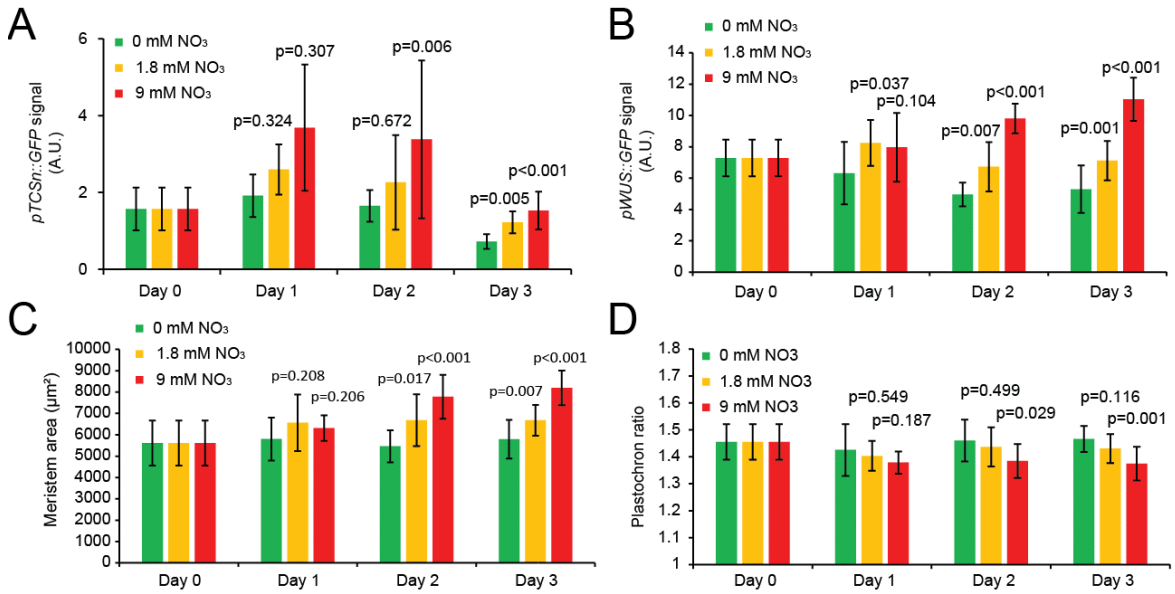

Fig. S12 Nitrate availability modulates meristem homeostasis

Effect of a transient nitrate treatment on the expression of *pTCSn::GFP* (*A*), the expression of *pWUS::GFP* (*B*), the size of the meristem (*C*) and the plastochron ratio (*D*) from independent experiments different from the ones presented in Fig.6 *A* to *C*. The treatments were performed at day 0 and different meristems were dissected and imaged each day (n=8-12). The different conditions were compared using Student's t-test. Error bars correspond to the mean ± SD.

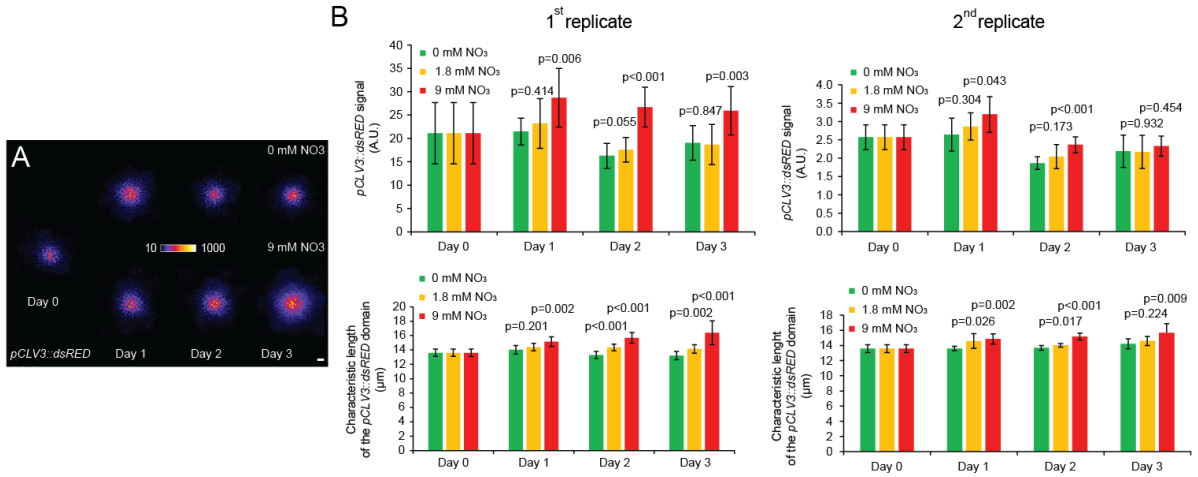

Fig. S13 Nitrate modulates the size of *CLV3* expression domain
(A) Representative meristems expressing *pCLV3::dsRED* from plants watered with 0 mM or 9 mM of NO3 (Scale bar: 10 µm). (*B*) Effect of transient the nitrate resupply on the expression level and on the size of the expression domain of *pCLV3::dsRED* in two independent experiments (n=8-12 meristems per day and per condition). The different conditions were compared using Student's t-test. Error bars correspond to the mean ± SD.

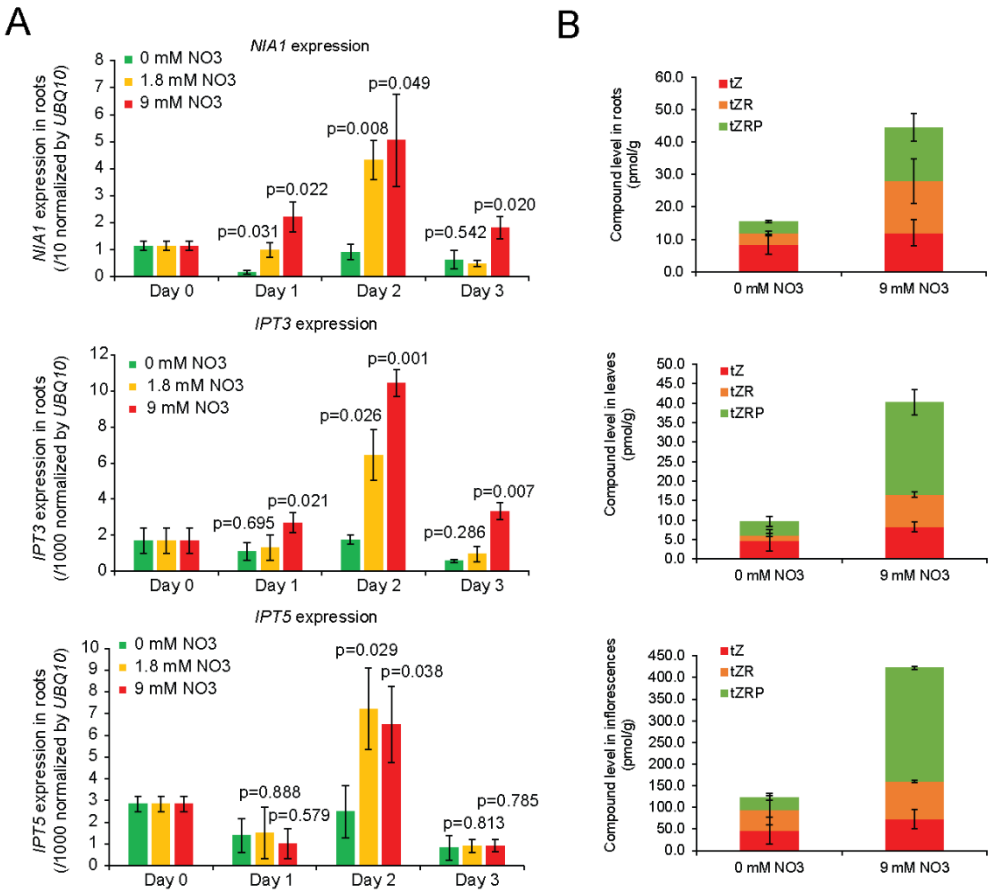

Fig. S14 Nitrate resupply leads to a transient activation of cytokinin biosynthesis
(*A*) Effect of the nitrate resupply on the expression of *NIA1* (a nitrate responsive gene), *IPT3* and *IPT5* in root tissues (3 replicates of 3 meristems each). The different conditions were compared using Student's t-test. Error bars correspond to the mean ± SD. (*B*) Concentration of tZRP, tZR and tZ species in root, leaf or inflorescence tissues measured 2 days after a treatment with a nutritive solution containing either 0mM of NO_3 or 9mM of NO_3 and measured by liquid chromatography mass spectrometry (3 replicates of 3 inflorescences each). Error bars correspond to the mean ± SEM.

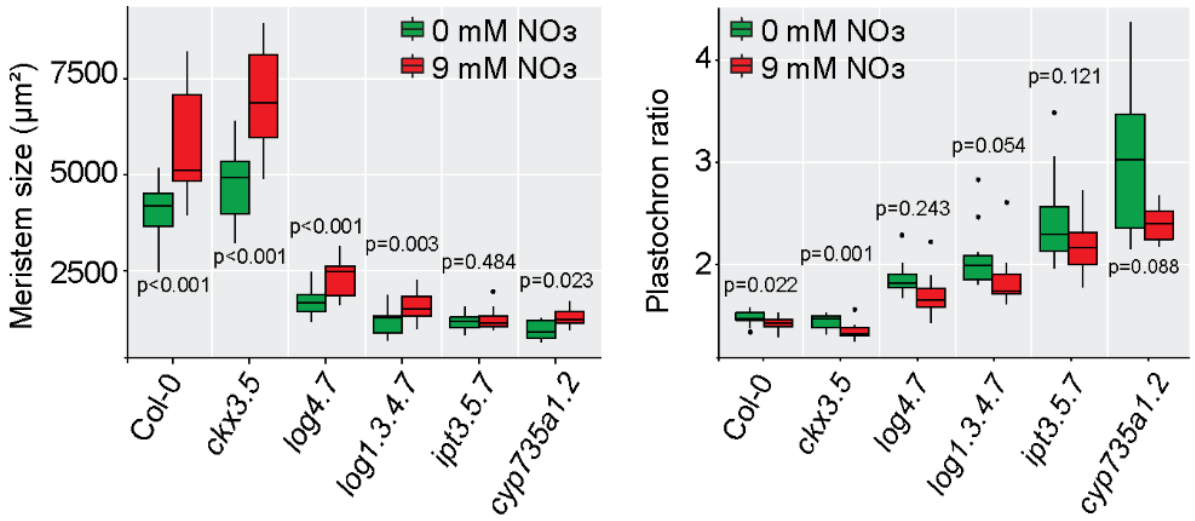

Fig. S15 SAM Response to NO_3 is reduced in *ipt3.5.7* mutant

Meristem size and plastochron ratio of WT and cytokinin-associated mutants three days after treatment with a nutritive solution containing either 0 mM (g) or 9 mM of NO_3 (r) from an independent experiment different from the one shown in Fig.6*D* (Col-0: n= 15 (g) and 15 (r), *ckx3.5*: n= 16 (g) and 15 (r), *log4.7*: n= 18 (g) and 14 (r), *log1.3.4.7*: n= 13 (g) and 15 (r), *ipt3.5.7*: n= 12 (g) and 13 (r), *cyp735a1.2*: n= 7 (g) and 8 (r)). Conditions were compared using Student's t-test. Error bars correspond to the mean ± SD.

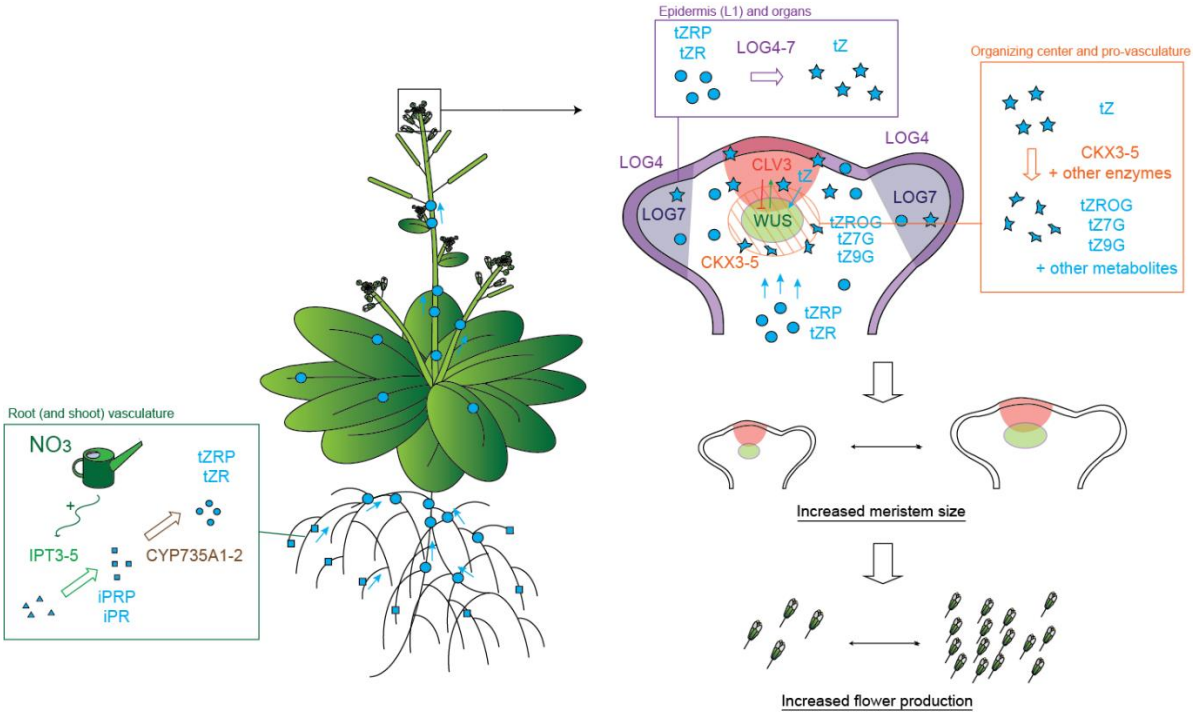

Fig. S16 An integrative and mechanistic model of the modulation of meristem function by nitrate
In the root predominantly, but also in the shoot, nitrate signaling induces the expression of *IPT3* and to a lesser extent expression of *IPT5* and thus the production of iP-type of cytokinin precursors (iPRP that can be converted to iPR). Those iP-type of cytokinin precursors are converted into tZ-type of cytokinin precursors (tZRP that can be converted to tZR) by CYP735A1 and 2 enzymes. Cytokinin precursors can then travel through xylem to the meristem. In the meristem, LOG4 activity in the epidermis and LOG7 activity in the organs trigger the production of active cytokinins (tZ) from the precursors. Active cytokinin acts positively on *WUS* expression. Active cytokinin can be inactivated (notably through glycosylation to produce tZROG, tZ7G, tZ9G) through various enzymatic activities including the activity of CKX enzymes (CKX3 and CKX5). WUS activity results in the induction of *CLV3* expression, the expansion of the stem cell domain, and thereby enlargement of the meristem and an increase of the rate of organ production.

Tab. S1 Comparison of the content in mineral nutrients of various types of soil.

Element (mg/L)	**Nitrate-N**	**Ammonia**	**Phosphorus**	**Potassium**	**Magnesium**	**Calcium**	**Sodium**
1/2 Soil 1/2 Sand	22.9 ± 3.6	20.3 ± 2.0	21.7 ± 2.3	87.0 ± 6.8	6.9 ± 2.3	10.5 ± 2.4	39.7 ± 2.8
1/1 Soil	51.0 ± 13.8	32.0 ± 10.0	52.43 ± 18.0	158.2 ± 24.1	34.5 ± 22.7	30.0 ± 16.1	51.9 ± 6.8
1/1 Soil + Fertilizer	557.5 ± 13.5	98.1 ± 10.3	323.0 ± 9.11	623.7 ± 11.5	193.6 ± 4.7	147.8 ± 8.2	288.3 ± 5.4

Element (mg/L)	**Sulphate**	**Boron**	**Copper**	**Manganese**	**Zinc**	**Iron**	**Chloride**
1/2 Soil 1/2 Sand	160.4 ± 16.3	0.13 ± 0.01	0.04 ± 0.01	0.12 ± 0.01	0.10 ± 0.01	31.87 ± 3.77	41.2 ± 8.0
1/1 Soil	296.4 ± 113.3	0.16 ± 0.05	0.04 ± 0.01	0.16 ± 0.09	0.19 ± 0.11	0.48 ± 0.06	58.1 ± 8.0
1/1 Soil + Fertilizer	417.1 ± 61.3	0.18 ± 0.01	0.05 ± 0.01	1.34 ± 0.03	0.49 ± 0.02	4.18 ± 0.07	105.7 ± 2.4

Mean ± SD concentration of mineral nutrients (mg/L) in different types of soil (½ Soil and ½ Sand, 1/1 Soil, 1/1 Soil + Fertilizer, 3 replicates) harvested from an experiment where plants were growing until bolting stage.

Tab. S2 Effect of nutrition on the concentration of different cytokinin species (First repeat)

Compound (pmol/g)	**tZ**	**tZR**	**tZRP**	**tZ7G**	**tZ9G**	**tZOG**	**tZROG**	**cZ**	**cZR**
Soil	85.0 ± 46.0	55.2 ± 8.0	108.5 ± 13.7	19.1 ± 1.5	5.7 ± 0.2	5.3 ± 0.4	3.0 ± 0.0	18.2 ± 6.9	7.1 ± 1.9
Soil + Fertilizer	16.4 ± 3.5	139.8 ± 20.1	243.9 ± 40.2	35.3 ± 2.6	7.8 ± 0.7	8.6 ± 1.4	11.1 ± 1.8	6.1 ± 3.2	6.1 ± 0.3
p-value	*0.274*	*0.038*	*0.065*	*0.011*	*0.096*	*0.134*	*0.044*	*0.217*	*0.656*

Compound (pmol/g)	**cZRP**	**cZ7G**	**DZ**	**DZR**	**DZ7G**	**IP**	**IPR**	**IPRP**	**IP9G**
Soil	17.5 ± 2.9	7.3 ± 1.3	1.9 ± 0.5	4.5 ± 2.5	11.4 ± 3.8	6.1 ± 3.7	6.9 ± 1.5	78.1 ± 7.3	3.6 ± 0.4
Soil + Fertilizer	20.0 ± 3.6	5.8 ± 1.8	1.0 ± 0.4	5.2 ± 0.5	13.6 ± 4.7	8.1 ± 6.2	8.5 ± 1.2	77.8 ± 19.3	2.9 ± 0.3
p-value	*0.621*	*0.541*	*0.267*	*0.803*	*0.734*	*0.805*	*0.457*	*0.989*	*0.270*

Mean ± SEM concentration of various cytokinin species (pmol/g) in inflorescences of plants grown on soil without or with fertilizer and measured by liquid chromatography mass spectrometry (n=3 replicates or 3 inflorescences each). Data were compared using Student tests.

Tab. S3 Effect of nutrition on the concentration of different cytokinin species (Second repeat)

Compound (pmol/g)	**tZ**	**tZR**	**ZRP**	**ZROG**	**cZR**	**cZRP**
1/1 Soil	23.3 ± 3.8	24.9 ± 11.1	527.6 ± 189.2	21.1 ± 7.9	1.3 ± 0.4	37.4 ± 14.4
1/1 Soil + Fertilizer	27.4 ± 9.9	98.4 ± 15.2	816.4 ± 216.7	53.8 ± 5.5	3.4 ± 1.2	52.4 ± 14.2
p-value	*0.726*	*0.021*	*0.373*	*0.033*	*0.212*	*0.497*

Compound (pmol/g)	**DZ**	**DZR**	**DZRP**	**IP**	**IPRP**	**IPR**
1/1 Soil	3.2 ± 0.7	10.6 ± 1.7	37.1 ± 14.2	1.2 ± 0.3	111.1 ± 31.5	0.9 ± 0.3
1/1 Soil + Fertilizer	4.0 ± 1.2	6.7 ± 1.5	70.2 ± 23.2	1.0 ± 0.4	212.0 ± 67.3	1.3 ± 0.3
p-value	*0.588*	*0.169*	*0.303*	*0.715*	*0.272*	*0.441*

Mean ± SEM concentration of various cytokinin species (pmol/g) in inflorescences of plants grown on soil without or with fertilizer and measured by liquid chromatography mass spectrometry from an independent experiment different from the one shown in Tab. S2 (n=3 replicates or 3 inflorescences each). Data were compared using Student tests.

Tab. S4 Effect of nitrate resupply on the concentration of different cytokinin species

Tissue	**Compound (pmol/g)**	**tZ**	**tZR**	**tZRP**	**tZ7G**	**tZ9G**	**tZOG**	**tZROG**	**cZ**	**cZR**
Roots	0mM NO_3	8.2 ± 2.9	3.7 ± 0.5	3.4 ± 0.4	38.4 ± 4.0	15.6 ± 1.5	2.7 ± 0.2	0.9 ± 0.1	11.7 ± 1.4	3.2 ± 0.2
	9mM NO_3	12.0 ± 4.0	15.9 ± 6.8	16.5 ± 4.3	58.4 ± 12.6	24.0 ± 5.0	2.9 ± 1.0	0.9 ± 0.3	12.3 ± 4.5	2.7 ± 0.4
	p-value	*0.502*	*0.213*	*0.091*	*0.248*	*0.228*	*0.814*	*0.873*	*0.913*	*0.361*
Leaves	0mM NO_3	4.7 ± 2.7	1.4 ± 0.4	3.5 ± 1.2	86.5 ± 7.1	22.4 ± 0.9	9.2 ± 1.0	2.5 ± 0.1	6.3 ± 1.8	3.5 ± 0.4
	9mM NO_3	8.3 ± 1.2	8.2 ± 0.7	23.8 ± 3.3	111.6 ± 2.5	27.2 ± 1.1	14.7 ± 0.7	3.6 ± 0.3	5.7 ± 0.2	5.7 ± 0.5
	p-value	*0.324*	*0.002*	*0.016*	*0.058*	*0.029*	*0.014*	*0.047*	*0.756*	*0.036*
Inflorescences	0mM NO_3	46.5 ± 31.0	48.6 ± 36.4	26.8 ± 5.3	21.9 ± 4.5	7.1 ± 1.4	2.4 ± 0.4	1.4 ± 0.2	4.2 ± 0.8	6.7 ± 1.8
	9mM NO_3	73.1 ± 21.8	87.0 ± 2.8	262.1 ± 3.1	114.6 ± 2.0	33.0 ± 0.9	12.5 ± 0.1	9.6 ± 0.1	3.2 ± 0.3	5.9 ± 0.3
	p-value	*0.526*	*0.402*	*<0.001*	*<0.001*	*<0.001*	*0.001*	*<0.001*	*0.317*	*0.710*

Tissue	**Compound (pmol/g)**	**cZRP**	**cZ7G**	**DZ**	**DZR**	**DZ7G**	**IP**	**IPR**	**IPRP**	**IP9G**
Roots	0mM NO_3	1.99 ± 0.0	71.8 ± 3.9	0.4 ± 0.1	1.1 ± 0.1	1.9 ± 0.2	1.6 ± 0.1	2.8 ± 0.1	18.3 ± 1.5	36.0 ± 5.1
	9mM NO_3	2.0 ± 0.1	54.6 ± 2.2	0.4 ± 0.1	1.6 ± 0.3	2.0 ± 0.3	2.4 ± 1.1	3.4 ± 1.0	18.3 ± 4.2	23.0 ± 7.0
	p-value	*0.775*	*0.027*	*0.761*	*0.230*	*0.754*	*0.539*	*0.619*	*0.991*	*0.214*
Leaves	0mM NO_3	3.3 ± 0.3	34.0 ± 1.7	1.6 ± 0.3	22.3 ± 1.7	5.4 ± 0.3	0.5 ± 0.1	1.2 ± 0.1	22.0 ± 2.3	10.0 ± 0.7
	9mM NO_3	6.8 ± 0.9	21.3 ± 0.8	1.4 ± 0.1	12.6 ± 0.3	5.7 ± 0.2	0.3 ± 0.0	1.4 ± 0.1	29.5 ± 2.4	9.2 ± 0.1
	p-value	*0.049*	*0.007*	*0.678*	*0.027*	*0.413*	*0.249*	*0.174*	*0.084*	*0.394*
Inflorescences	0mM NO_3	9.7 ± 1.7	5.7 ± 1.2	1.2 ± 0.2	11.5 ± 1.7	1.6 ± 0.4	1.4 ± 0.7	2.1 ± 0.6	33.2 ± 2.0	1.8 ± 0.2
	9mM NO_3	14.7 ± 0.3	6.4 ± 0.0	1.4 ± 0.1	15.4 ± 1.0	7.3 ± 0.3	1.4 ± 0.8	2.6 ± 0.4	70.2 ± 1.2	2.9 ± 0.3
	p-value	*0.095*	*0.638*	*0.432*	*0.133*	*<0.001*	*0.990*	*0.490*	*<0.001*	*0.043*

Mean ± SEM concentration of various cytokinin species (pmol/g) in root, leaf or inflorescence tissues measured 2 days after a treatment with a nutritive solution containing either 0mM of NO_3 or 9mM of NO_3 and measured by liquid chromatography mass spectrometry (3 replicates of 3 inflorescences each). The different conditions were compared using Student's t-test.